

## SOME REFORMATIVE TRIALS OF PIEZO-MOTORS USING LONGITUDINAL AND FLEXURAL VIBRATIONS

**Y. Tomikawa<sup>1</sup>, T. Funakubo<sup>1,2</sup>, O. Miyazawa<sup>3</sup>, M. Aoyagi<sup>1</sup> and T. Takano<sup>4</sup>**

<sup>1</sup> Graduate Program of Systems and Information Engineering, Group of Electro-Mechanical Engineering,  
Yamagata University, Yamagata, JAPAN

<sup>2</sup> Integrate Precision Technology Department, Olympus Optical Co. Ltd., Tokyo, JAPAN

<sup>3</sup> Project Promotion Group, FX Promotion Department of Seiko Epson Co. Ltd., Nagano, JAPAN

<sup>4</sup> Department of Communication Engineering, Tohoku Institute of Technology, Miyagi, JAPAN  
tomikawa@yz.yamagata-u.ac.jp

### Abstract

This paper deals with 4 reformative trials of piezo-motors using longitudinal and flexural vibrations. The purpose of these trials is to further promote applications of an ultrasonic motor. This is because this type of motor is basically composed of a rectangular plate, and therefore it is very simple to construct and has become a popular ultrasonic motor. Considering these situations, we have continued to study this type of an ultrasonic motor; that is, the contents of this paper are some results performed recently in the study.

Keywords: Ultrasonic motor, Piezoelectric vibration, Longitudinal vibration, Flexural vibration, Linear motor, Piezoelectric ceramics, Multiple piezoelectric actuator

### 1. Introduction

We have contributed to development of an ultrasonic motor and its practical application to some extent until now. However, specific features of an ultrasonic motor are not enough drawn and their effectiveness are not sufficiently recognized in the engineering.

Therefore, in order to further promote application of an ultrasonic, continuous studies of it must be done, because it is much expected to be a key-device in the nanometer technology of next stage. Depending upon such thought, we continue to study some types of an ultrasonic motor, and so in this paper we would like to present our reformative trials of an ultrasonic motor, which were done recently. That is, the contents of such trials are as follows:

- (1) 10mm size ultrasonic linear motor using multi-layer piezoelectric actuator made of hard material.
- (2) Application of a  $L_1$ - $F_2$  double mode ultrasonic motor to a micro-robot "Mush II -P".
- (3) High-speed rotary-type ultrasonic motor of thin makes.
- (4) Ultrasonic motor using a  $L_1$ - $F_2$  double mode piezoelectric vibrator with T-form cross-section.

### 2. 10mm Size Ultrasonic Linear Motor Using Multi-layer Piezoelectric Actuator Made of Hard Material

#### a. 10mm Size Ultrasonic Motor Using Multi-layer Piezoelectric Actuator

When a moving element of a small piece of equipment must be linearly driven, an ultrasonic linear motor is among the most suitable candidate actuators. An  $L_1$ - $F_2$  mode vibrator is a typical vibrator for use in an ultrasonic linear motor. In an  $L_1$ - $F_2$  mode vibrator, a first longitudinal mode and a second flexural mode are simultaneously excited in a rectangular parallelepiped elastic body, and an elliptical motion of displacement is produced at some particular portions of the elastic body.

Recently, a low-voltage-drive-ultrasonic linear motor is required. Therefore, such a linear motor applying multilayer piezoelectric actuators as shown in Fig.2.1, has been developed. That is, the 10mm size motor is such that the size of the stator vibrator is  $10\text{mm} \times 2.5\text{mm} \times 2.0\text{mm}$ , as shown in Fig.2.2, driving voltage is  $5V_{rms}$ , Maximum thrust force is 0.7N and maximum speed is 120mm/sec.

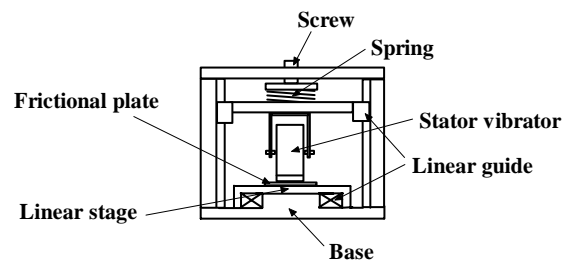


Fig.2.1 Prototype linear motor.

The reason why such 10mm size motor has been developed is as follows: In recent years, many devices and instruments, such as micro-factories and micro-manipulators, are expected to be small and to be driven at fairly low voltages. That is, in an attempt to reduce the size of the  $L_1$ - $F_2$  mode vibrator while maintaining low voltage drive characteristics, we fabricated a multilayer  $L_1$ - $F_2$  mode vibrator as shown in Fig.2.2.

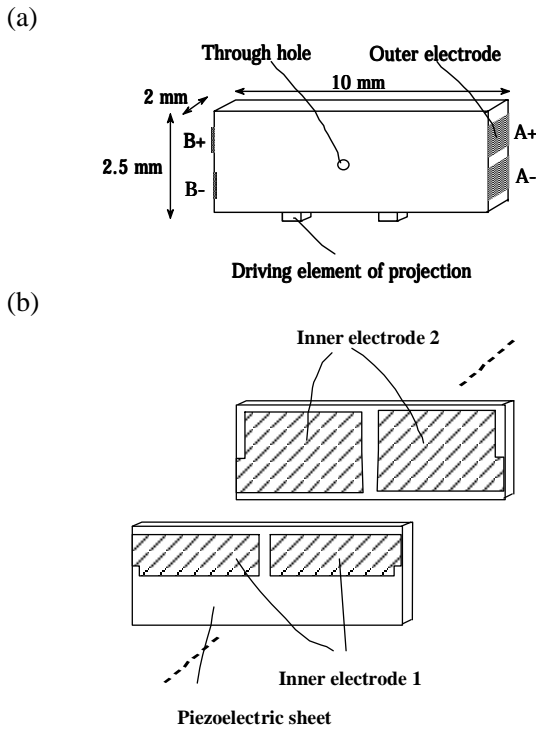


Fig.2.2 Multilayer  $L_1$ - $F_2$  mode vibrator (a) schematic view (b) inner electrode patterns.

Figure 2.2 shows a schematic view of the multilayer vibrator. The multilayer vibrator has a rectangular parallelepiped shape and a width of 10mm, a height of 2.5mm, and a depth of 2mm. Two pairs of outer electrodes (A+, A- and B+, B-) are affixed on the side surface of the vibrator. Two driving elements of projection are fixed at positions on the lower surface of the vibrator where elliptical motions of displacement are generated. The electromechanical coupling factor  $k_{31}$  and the mechanical quality factor  $Q_m$  of the piezoelectric sheet are 33(%) and 1060, respectively. Inner electrodes are printed on the surface of the piezoelectric greensheets. As shown in Fig.2.2, each inner electrode 1, which serves as a positive electrode, is divided into two equal areas on the upper half area of the piezoelectric sheet, and in each of the two areas, one part of the inner electrode 1 is extended to the edge of the corresponding piezoelectric sheet where the inner electrode 1 comes in contact with the outer electrode A+ or B+. Inner electrode 2, which serves as a negative electrode, is also divided into two equal areas on the area of the piezoelectric sheet. As shown in Fig.2.2, these piezoelectric sheets with inner electrodes 1 and inner electrode 2 are alternately stacked in the depth (2mm) direction. Each piezoelectric sheet has a thickness of 80  $\mu\text{m}$ , and 25 piezoelectric sheets are provided. Then they are fired in the electric furnace, and then the outer electrodes are affixed on the surface of the multilayer vibrator. Thereafter, polling is performed by applying a high voltage between A+ and A-, and between B+ and B-.

Areas of the piezoelectric sheets where inner electrodes do not exist are directly contacted to each other by stacking.

Here we refer to the reason why inner electrodes are divided into two instead of into four. First, in the case that inner electrode 1 is divided into two as described above, the height of the inner electrode 1 is 0.85mm. On the other hand, in the case that the inner electrode 1 is divided into four, the height of the inner electrode 1 will be 0.65mm, because an insulating space of 0.4mm is required between the upper and the lower half areas of the inner electrode 1. As a result, the effective area of inner electrode 1 in the case of dividing into four is not always twice as large as that in the case of dividing into two. Second, four outer electrodes are required in the case of dividing into two as described above. On the other hand, six outer electrodes are required in the case of dividing into four. Therefore, in the case of dividing into four, the outer electrodes must be set up not only on the side surface but also on the upper or lower surface in the vibrator.

**b. Characteristics of Multilayer Piezoelectric Vibrator**

**(1) Electro-mechanical characteristics**

The electromechanical coupling factor  $k$  ( $k$  factor) of the vibrator was calculated by the following formula,  $k_2=1/\gamma+1$ , where  $\gamma=C_0/C$  is the capacitance ratio. The mechanical quality factor  $Q$  ( $Q$  factor) of the vibrator is defined as a  $Q$  value calculated in the series resonance circuit of the equivalent circuit. Figure 2.3 shows the measured results. The  $k$  factor of the longitudinal mode is greater than that of the flexural mode. The  $k$  factors of the longitudinal mode and the flexural mode increase slightly with the amplitude of the applied voltage. The  $Q$  factor of the longitudinal mode and the flexural mode are approximately equal and decrease monotonically with increasing amplitude of the applied voltage. In addition, the reason why no data are obtained above 9  $V_{p-p}$  in the longitudinal mode is that a jumping phenomenon of the impedance curve occurs when the measuring voltage is above 9  $V_{p-p}$ .

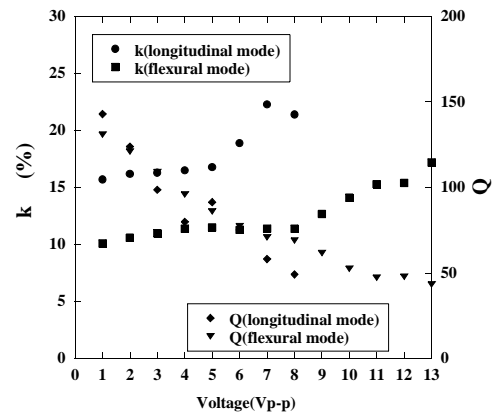


Fig.2.3 Driving voltage dependence of  $k$ -factor and  $Q$ -factor of multilayer  $L_1$ - $F_2$  mode vibrator.

(2) Vibration Velocity and Temperature Rise of Multilayer Vibrator

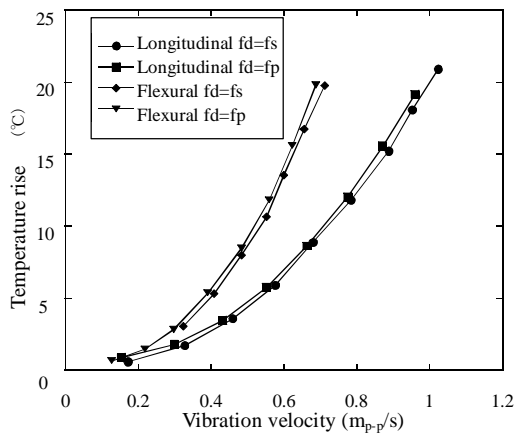


Fig.2.4 Temperature rise vs. vibration velocity of multilayer L<sub>1</sub>-F<sub>2</sub> mode vibrator.

In Fig.2.4,  $f_d$  represents driving frequency,  $f_s$  represents series resonance frequency, and  $f_p$  represents parallel resonance frequency. In the longitudinal mode, the temperature rises by 20°C when the vibration velocity reaches about 1 m<sub>p-p</sub>/s, at both the series resonance frequency and the parallel resonance frequency. In the flexural mode, the temperature rises by 20°C when the vibration velocity reaches about 0.7 m<sub>p-p</sub>/s, at both the series resonance frequency and the parallel resonance frequency. Hence, at a given vibration velocity, the longitudinal mode generates less heat than the flexural mode.

c. Characteristics of Prototype Motor

In Fig.2.1, the vibrator is pressed to the linear stage by a screw and a spring, at a force of about 3 N. A friction plate made of zirconia ceramics is prepared on the linear stage. When alternating voltages are applied to the A-phase (A+, A-) and the B-phase (B+, B-) at resonance frequency with a phase difference of  $\pi/2$ , elliptical motions of displacement are generated at the positions of the driving element of projections of the vibrator. Thereafter, the linear stage moves back and forth linearly.

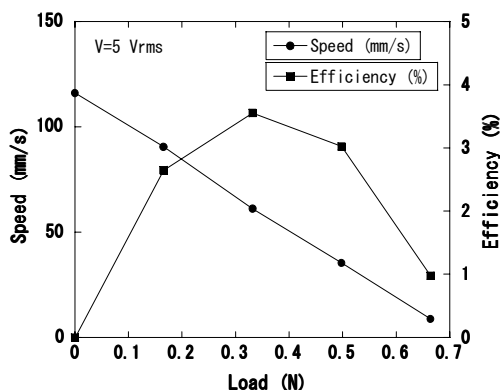


Fig.2.5 Speed vs. load characteristics.

Figure 2.5 shows the relationship between load and speed, and the relationship between load and efficiency for an applied voltage of 5 V<sub>rms</sub>. Maximum thrust force is about 0.7N, maximum speed is about 120 mm/s, and maximum efficiency is about 4%. Additionally, input power is about 0.6W. Figure 2.6 shows one example of the linear movement characteristics measured with use of the optical linear encoder.

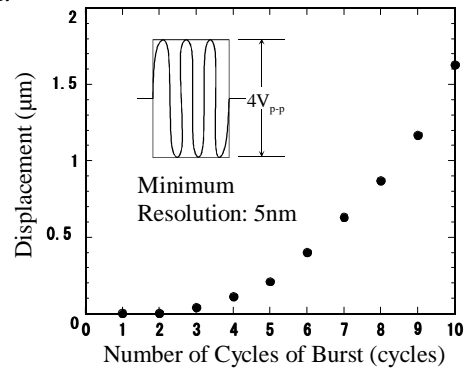


Fig.2.6 Displacement characteristics.

d. Summary

- (1) The multilayer L<sub>1</sub>-F<sub>2</sub> mode vibrator whose inner electrodes are simply divided into two can excite a first longitudinal mode and a second flexural mode.
- (2) The electromechanical coupling factor  $k$  was found to increase with increasing applied voltage and the mechanical quality factor  $Q$  was found to decrease monotonically with increasing applied voltage.
- (3) The multilayer L<sub>1</sub>-F<sub>2</sub> mode vibrator exhibited a sufficiently large amplitude of vibration velocity when temperature rose by 20°C.
- (4) An ultrasonic linear motor using such a multilayer L<sub>1</sub>-F<sub>2</sub> mode vibrator exhibited superior performance characteristics in practical application.

3. Application of a L<sub>1</sub>-F<sub>2</sub> Mode Ultrasonic Motor to a Micro-Robot “Mush II -P”



Fig.3.1 Wheel module.

As an application of very small ultrasonic motor, such a trial as shown in Fig.3.1 has been done, by Dr. O. Miyazawa and his research group of Seiko Epson Co. Ltd. That is, the research group has developed a micro-robot named “Mush II -P”, which is one of a series of micro-robot “Mush”, and in the robot they

applied the very small ultrasonic motor shown in Fig.3.11 to bear a driving force of wheels installed. The motor is constructed using a longitudinal ( $L_1$ ) and flexural ( $F_2$ ) double mode piezoelectric ceramic vibrator, as shown in Fig.3.2.



Fig.3.2 Stator vibrator.

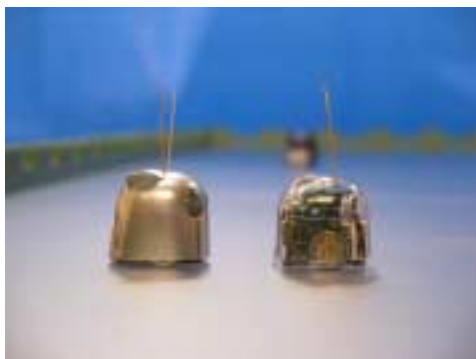


Fig.3.3 Photo. of Micro-Robot "Mush II -P".

The micro-robot "Mush II -P" is as shown in Fig.3.3, where two blue-tooth modules using very small motor as shown in Fig.3.1 are installed and these modules make possible free and smooth movement of the robot "Mush".

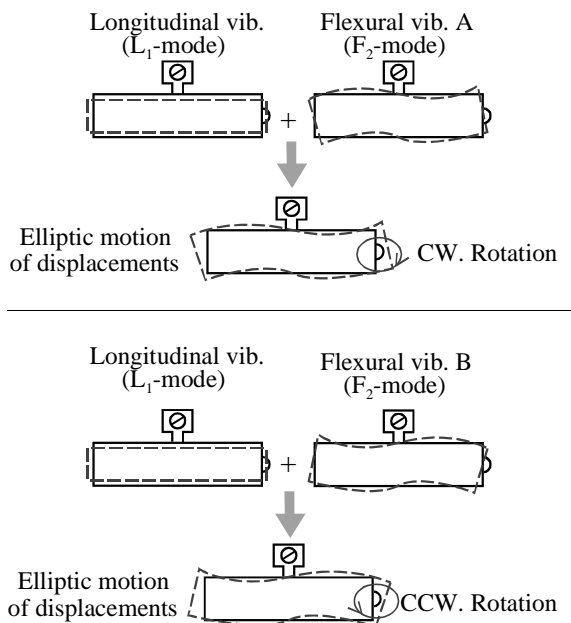


Fig.3.4  $L_1$ - $F_2$  double mode PZT stator vibrator for elliptic motion of displacements.

**Special features of very thin type ultrasonic motor**

**Operation principle of the motor**

- 1) Forming of elliptic motion of displacement by piezo-ceramics stator vibrator
- 2) Revolution of wheel driven by friction torque due to elliptic motion of displacement

**Merits of the motor**

- Very thin construction : stator thickness=0.4mm  
wheel diameter/thickness=11mm/2mm
- Flexibility of construction : driving other part except wheel is possible, and installation of driving parts is easy and simple
- Wide range setting of torque: same stator vibrator can give a wide range of torque

**Input/output characteristics of the motor**

• Driving voltage: 2.2V	Maximum driving force: 2gf
• Input power : 26mW	Maximum revolution speed: 200mm/sec

Fig.3.5 Ultrasonic motor practically used in small robot "Mush II -P" and special features of its blue-tooth modules.

Operation principle of the ultrasonic motor is shown in Fig.3.4. This principle is same as conventional one, but the fabrication is great because it can skillfully be done using watch technology. The features of this blue-tooth module using a  $L_1$ - $F_2$  mode ultrasonic motor are shown in Fig.3.5, and moreover, measured characteristics of the motor-module are shown in Figs.3.6 and 3.7 respectively. Figure 3.8 shows fantastic scenes "Micro-robot Theater", demonstrated in the robot-show held in April 2003 at Yokohama, Japan. In the theater, some micro-robots "Mush II -P" can play funny and pleasant dances, under outer electrical and mechanical controlling to them.

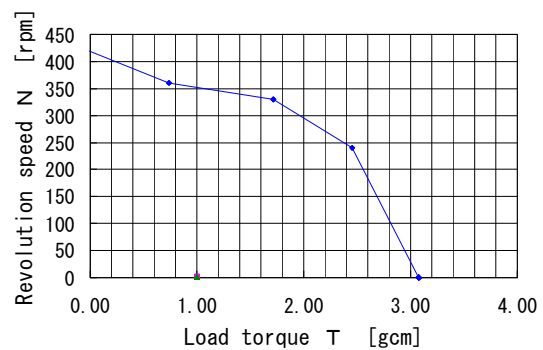


Fig.3.6 Measured characteristics of wheel module.

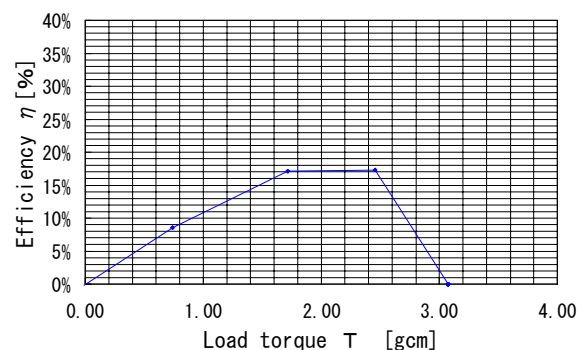


Fig.3.7 Measured characteristics of wheel module.



Fig.3.8 A scene of Robot-Theater demonstrated at the “robot-show”.

**4. High-Speed Rotary-Type Ultrasonic Motor of Thin Makes**

In Yamagata University, as a challenge to a new field of an ultrasonic motor, the motor with fine performance of high revolution speed has been studied in order to apply it to a micro fan, micro pump and so on. The ultrasonic motor proposed for such application is to use longitudinal-flexural coupling-vibration mode of a thin plate with a vibratory piece.

**a. Construction**

The basic configuration of this motor is shown in Fig.4.1, where the stator vibrator consists of a metal plate (thickness 0.2 mm) sandwiched by two thin piezoelectric ceramic plates (thickness 0.3 mm) of which electrode are not divided, and this ultrasonic motor can be driven by single ac source. In order to achieve a high revolution speed, a slender rotary shaft of diameter 1.5mm is used so that it is driven to rotate by picking motion of vibratory piece.

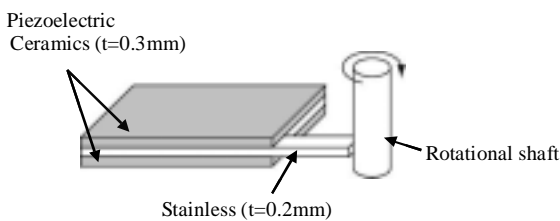


Fig.4.1 Basic configuration of proposed mode-conversion ultrasonic motor.

**b. Operation principle and vibration modes**

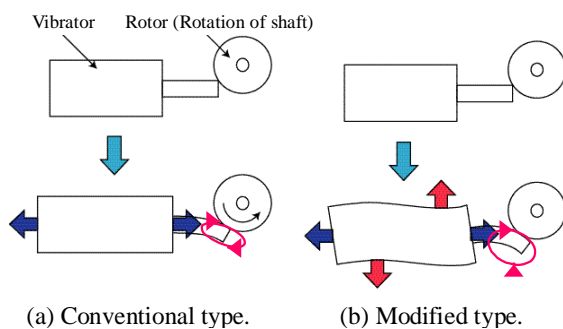


Fig.4.2 Operation principle of mode-conversion ultrasonic motors.

Operation principle of this motor is shown in Fig.4.2 (b); that is, in the motor proposed, not only mode-conversion from longitudinal vibration to flexural one on vibratory piece, but also coupling between longitudinal and flexural vibrations on the main stator vibrator are used. Concretely, three types of stator vibrators were investigated, as shown in Figs.4.3, 4.4 and 4.5. The former in Fig.4.3 can be called a longitudinal-flexural coupling vibrator type, and the latter is called a type of longitudinal-flexural coupling vibrator combined with velocity transformer; that is, in the latter type, two constructions of type-1 and type-2, as shown in Figs.4.4 and 4.5, respectively, can be considered.

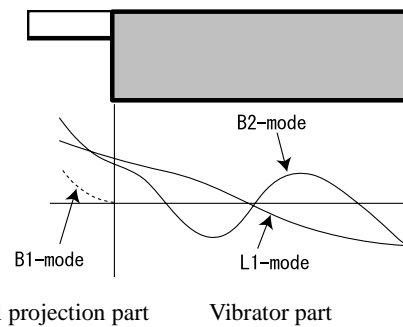


Fig.4.3. Vibration modes of longitudinal-flexural coupling vibrator.

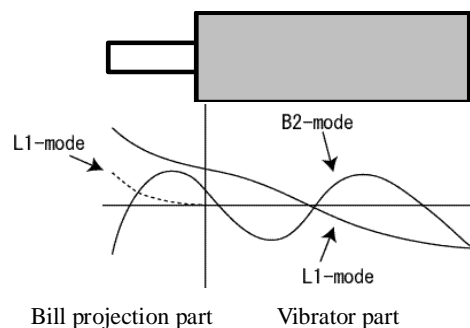


Fig.4.4. Vibration modes of longitudinal vibrator with a vibratory piece acting as velocity transformer (Type-1).

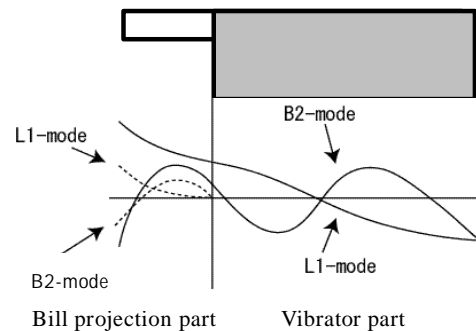
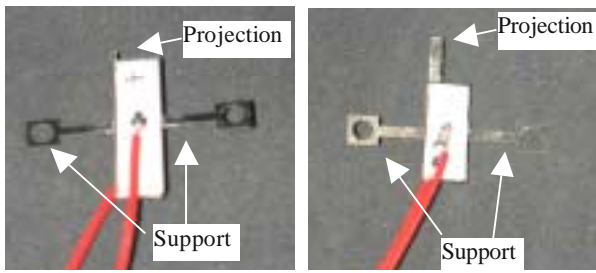


Fig.4.5. Vibration modes of longitudinal-bending coupling vibrator combined with velocity transformer (Type-2).

c. Prototype motors and their Characteristics



(a) Coupling vibrator. (b) Type-2.

Fig.4.6 Experimental stator vibrators used in the experiment.

Prototype stator vibrators of motors are shown in Figs.4.6 (a) and (b), where two support arms (length 5mm and width 1mm) are provided on both-sides of vibrator central portion and are clamped with screws. Dimensions of prototype stator vibrator are as follows:

<Coupling type>

Main Vibrator:  $L10.0 \times W4.0 \times T0.8 \text{ mm}^3$

Vibrator piece:  $Lt(1.2, 1.5, 2.5) \times Wc \times 0.5 \times T0.2 \text{ mm}^3$

<Velocity transform type (type-2)>

Main vibrator:  $L10.0 \times W4.0 \times T0.8 \text{ mm}^3$

Vibrator piece:  $L5.0 \times W1.1 \times T0.2 \text{ mm}^3$

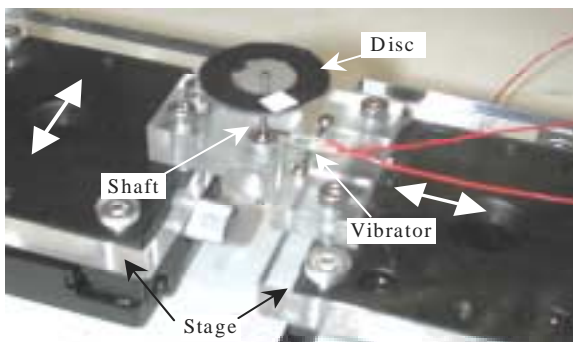


Fig.4.7 Experimental device.

Fig.4.7 shows whole motor equipped on the experimental apparatus to measure motor characteristics. In Fig.4.7 pressing of the stator vibrator to a rotary shaft and its adjusting can be done with moving the support-stage.

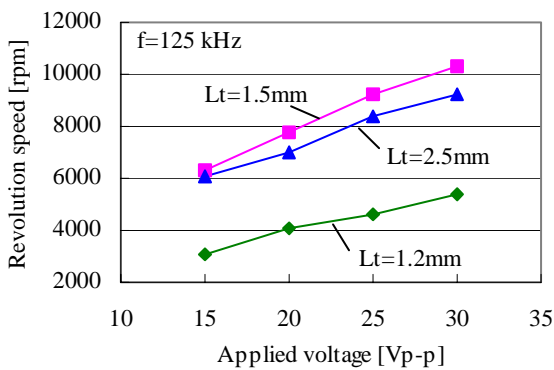


Fig.4.8 Revolution speed vs. applied voltage.

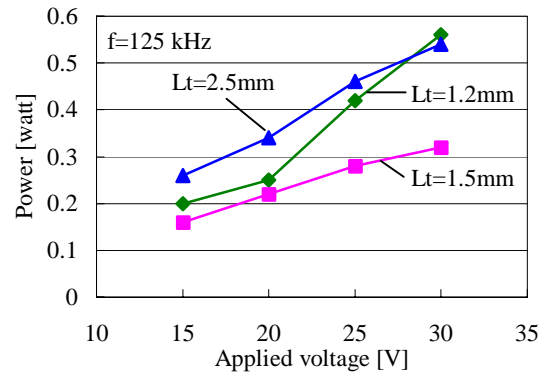


Fig.4.9 Power vs. applied voltage.

Measured motor characteristics of coupling type motor are shown in Figs.4.8 and 4.9; that is, in the case of  $Lt=1.5\text{mm}$  such motor characteristics as revolution speed 10,000 rpm at input voltage 30v-p and input power 0.3 watt was obtained. On the other hand, in the velocity transform motor of type-1 and 2, characteristics shown in Figs.4.10 and 4.11. In these motors, the type-2 motor could achieve a better characteristic of 10,000 rpm revolution speed at input voltage 30  $V_{p-p}$  and input power 0.4watt than the type-1.

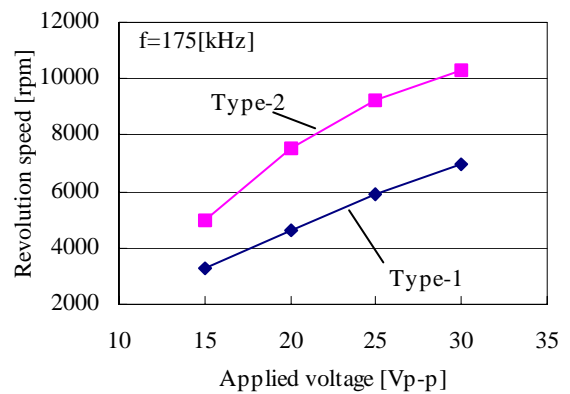


Fig.4.10 Revolution speed vs. applied voltage.

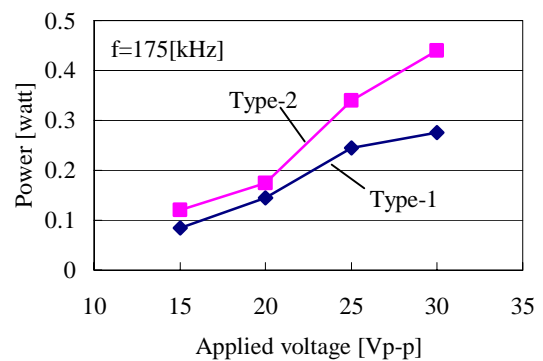


Fig.4.11 Power vs. applied voltage.

d. Summary

As a result, an ultrasonic motor of 0.8 mm thickness could rotate a shaft of 1.5mm diameter over 10,000 rpm under the conditions of applied voltage: 10V and input power: 0.3 watt.

**5. Ultrasonic Motor Using a  $L_1$ - $F_2$  Double Mode Piezoelectric Vibrator with T-form-Cross-Section**

**a. Construction of stator vibrator and its operation principle**

As mentioned in the above sections, the ultrasonic motor using a  $L_1$ - $F_2$  double mode piezoelectric vibrator is basically composed of a rectangular plate, in which the  $F_2$  mode has vibrational displacements in its surface plane; that is, this type of motor has such merits that the form is very simple, and thin form of an ultrasonic motor can be constructed and so on. However, only a defect found in the motor construction is that flexural vibration of the 2nd mode cannot be excited as strongly as the 1st longitudinal vibration mode. This is because the excitation is usually done by using the transverse effect of piezoelectric ceramics. It can be said that this defect might be not avoidable because it is concerned with the principle of piezoelectric-ceramic-vibration. However, in order to break through the defect, Y. Tomikawa, one of authors, has devised to construct a  $L_1$ - $F_2$  double mode vibrator with T-form cross-section, as shown in Fig.5.1. That is, it is thought that the  $L_1$ - $F_2$  double mode stator vibrator for an ultrasonic motor may operate as shown in Fig.5.2.

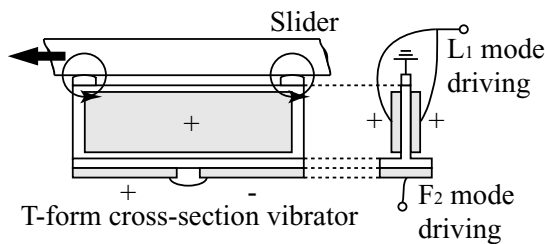


Fig.5.1  $L_1$ - $F_2$  double mode stator vibrator with T-form cross-section for linear actuator.

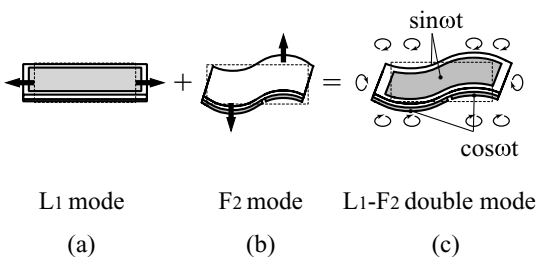


Fig.5.2 Elliptical motions on the  $L_1$ - $F_2$  mode stator vibrator of T-form cross-section.

**b. Simulation of vibrational Characteristics**

In order to make sure the effectiveness of this stator vibrator proposed, finite element method simulation was applied to the vibrators in Fig.5.3 and vibrational displacements in X and Y directions were obtained. From the results; it is found clear that by selection of

adequate dimensions, the displacement in the Y direction might be made larger than the one in the X direction, as shown in Fig.5.4.

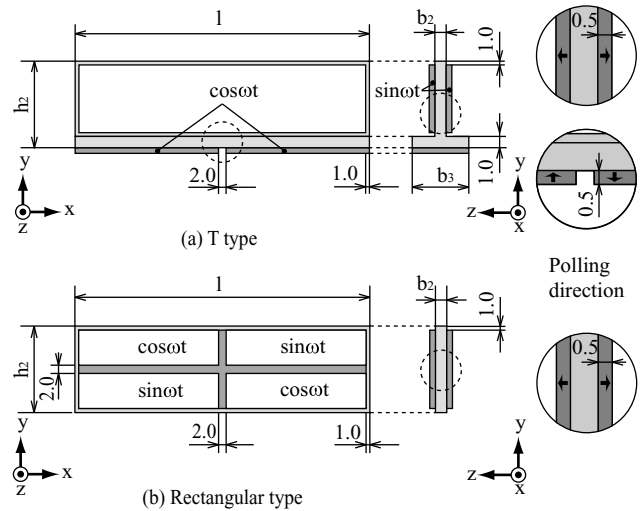


Fig.5.3 T-form cross-section  $L_1$ - $F_2$  mode vibrator for FEM simulation.

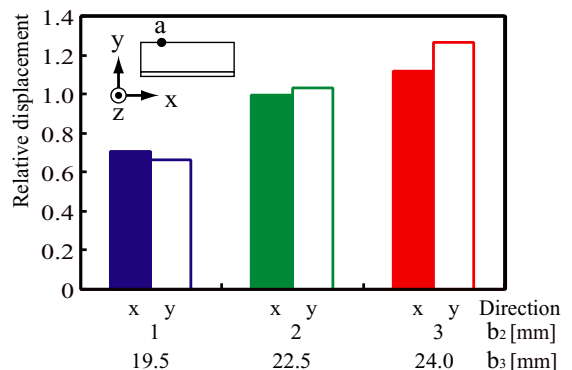
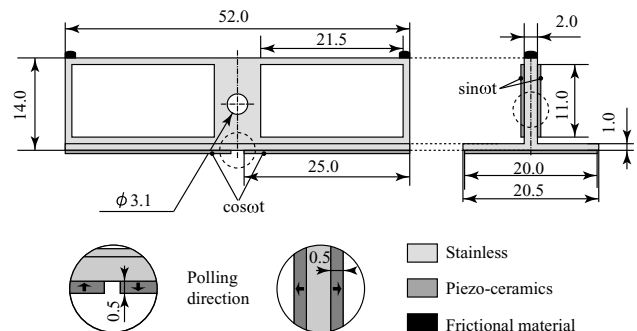
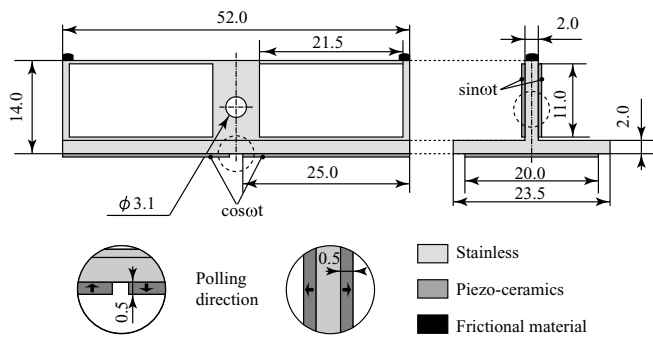


Fig.5.4 Simulated relative displacements of the vibrators in Fig.5.3 (a) and (b).

**c. Experiments**



(a) Type A vibrator



(b) Type B vibrator

Fig.5.5 T-form cross-section  $L_1$ - $F_2$  mode vibrators in the measurement.

In the experiments, two types of prototype vibrator (Type A and Type B) shown in Figs.5.5 (a) and (b) were measured. Table 5.1 shows comparison of measured characteristics between these modified T-form cross-section vibrators and the conventional vibrator shown in Fig.5.6.

Table 5.1 Ratio of motional admittance circle ( $Y_{F2}/Y_{L1}$ ) and ratio of coupling factor ( $k_{vF2}/k_{vL1}$ ).

	Ratio of Motional admittance circle ( $Y_{F2}/Y_{L1}$ )	Ratio of coupling factor ( $k_{vF2}/k_{vL1}$ )
Type A	1.202	1.339
Type B	0.691	1.369
Conventional type	0.342	0.591

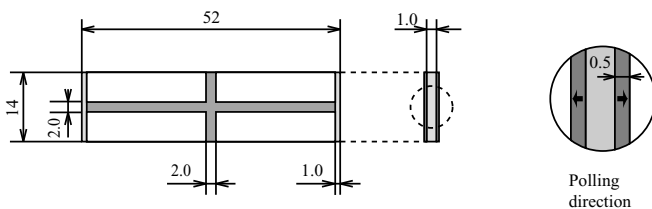


Fig.5.6 Conventional  $L_1$ - $F_2$  mode vibrator for comparison of measured vibrational characteristics.

From these results, it can be found that the  $F_2$  mode excitation relative to the  $L_1$ -mode one can be improved in the modified vibrator. This modified  $L_1$ - $F_2$  stator vibrator might be applied to construct the linear motor as shown in Fig.5.7; that is, this linear motor has two functions of large and small moving operation, in which the large operation is achieved by this modified  $L_1$ - $F_2$  mode stator vibrator. Figure 5.8 shows another application to construct a rotary motor, which is made as a trial as shown in Fig.5.9, with such measured characteristics as in Fig.5.10.

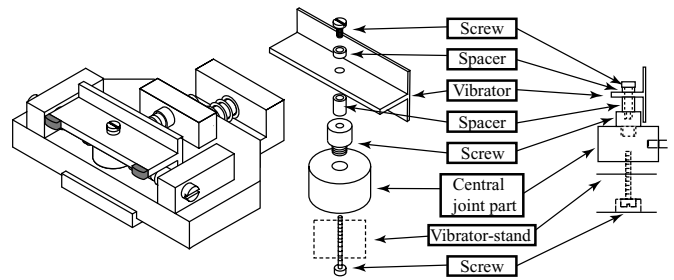


Fig.5.7 Linear actuator with two functions of large and small moving operation, using the T-form cross-section  $L_1$ - $F_2$  mode vibrator.

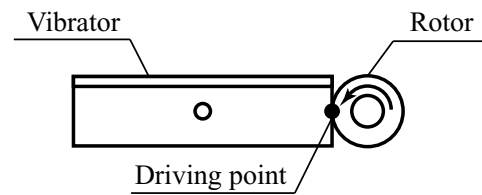


Fig.5.8 Application of the T-form cross-section  $L_1$ - $F_2$  mode vibrator to a rotary motor.

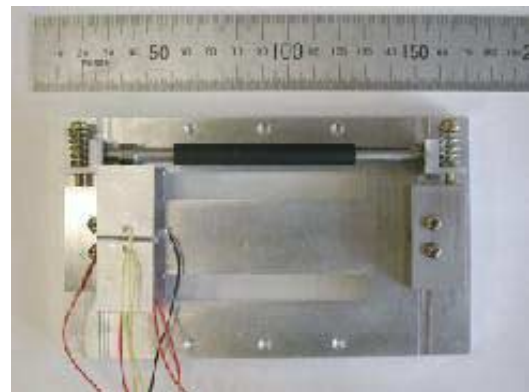


Fig.5.9 Construction of prototype motor shown in Fig.5.8.

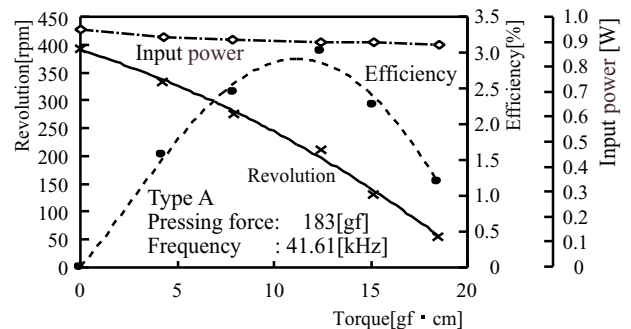


Fig.5.10 Measured characteristics of the motor shown in Fig.5.9.